Rapid and Sensitive Colorimetric ELISA using Silver Nanoparticles, Microwaves and Split Ring Resonator Structures

Sarah A. Addae[1], **Melissa A. Pinard**[1], **Humeyra Caglayan**[2], **Semih Cakmakyapan**[2], **Deniz Caliskan**[2], **Ekmel Ozbay**[2], and **Kadir Aslan**[*,1]

[1]Morgan State University, Department of Chemistry, Baltimore, MD, 21251, USA

[2]Bilkent University, Nanotechnology Research Center, Ankara, 06680, TURKEY

Abstract

We report a new approach to colorimetric Enzyme-Linked Immunosorbent Assay (ELISA) that reduces the total assay time to < 2 min and the lower-detection-limit by 100-fold based on absorbance readout. The new approach combines the use of silver nanoparticles, microwaves and split ring resonators (SRR). The SRR structure is comprised of a square frame of copper thin film (30 µm thick, 1 mm wide, overall length of ~9.4 mm on each side) with a single split on one side, which was deposited onto a circuit board (2×2 cm^2). A single micro-cuvette (10 µl volume capacity) was placed in the split of the SRR structures. Theoretical simulations predict that electric fields are focused in and above the micro-cuvette without the accumulation of electrical charge that breaks down the copper film. Subsequently, the walls and the bottom of the micro-cuvette were coated with silver nanoparticles using a modified Tollen's reaction scheme. The silver nanoparticles served as a mediator for the creation of thermal gradient between the bioassay medium and the silver surface, where the bioassay is constructed. Upon exposure to low power microwave heating, the bioassay medium in the micro-cuvette was rapidly and uniformly heated by the focused electric fields. In addition, the creation of thermal gradient resulted in the rapid assembly of the proteins on the surface of silver nanoparticles without denaturing the proteins. The proof-of-principle of the new approach to ELISA was demonstrated for the detection of a model protein (biotinylated-bovine serum albumin, b-BSA). In this regard, the detection of b-BSA with bulk concentrations (1 µM to 1 pM) was carried out on commercially available 96-well high throughput screening (HTS) plates and silver nanoparticle-deposited SRR structures at room temperature and with microwave heating, respectively. While the room temperature bioassay (without microwave heating) took 70 min to complete, the identical bioassay took < 2 min to complete using the SRR structures (with microwave heating). A lower detection limit of 0.01 nM for b-BSA (100-fold lower than room temperature ELISA) was observed using the SRR structures.

Keywords

Immunoassays; Bioassays; ELISA; Silver island films; Silver colloids

---

[*]Corresponding authors. Kadir.Aslan@morgan.edu.

1. Introduction

Currently two major limitations are encountered in ELISA used for the detection of biomolecules: rapidity of the bioassay and detection sensitivity. Rapidity is limited by the chemical kinetics involved during the binding of proteins, which typically takes several min to hours for each step in ELISA [1]. Sensitivity is affected by the quantum yield of chromophores for chemiluminescence-based detection, the narrow-range of signal for colorimetric (absorbance-based detection) and the inherent optical limitations of the detection system. Although chemiluminescence-based detection is more sensitive than the colorimetric detection [2], colorimetric ELISA is still in use due to simplicity of the detection system [2–4]. That is, the absorbance values at fixed wavelength can be accurately measured by relatively inexpensive detectors. Moreover, colorimetric sensing methodology can easily be adapted to portable devices [4]. Since the absorbance values are linear only between 0 and 1, one has to dilute the samples that have absorbance values >1, or employ additional steps to increase the signal for samples with low concentration of target molecule. Despite these efforts, the detection of low concentration of target molecule by colorimetric ELISA is still problematic. In this regard, there is a need to further improve the lower detection limit of colorimetric ELISA.

It was previously shown that the rapidity and sensitivity of fluorescence-based bioassays can be improved by the combined use of low-power microwave heating and plasmon-resonant particles (PSPs, e.g., silver nanoparticles) [5,6]. The improvement in the sensitivity of the bioassays is due the close-range interactions of fluorescent species with PSPs, where an increase in fluorescence signatures and a decrease in lifetimes of fluorophores are observed [7]. The rapidity was improved by low-power microwave heating of the bioassay components, where a thermal gradient between the assay medium and PSPs result in the completion of biorecognition events in less than 1 min [5]. Despite the usefulness of low-power microwave heating with PSPs for the construction of rapid bioassays, the issue of control over the uniform heating of small volume samples ($\leq 100\ \mu l$) remains unresolved. One has to employ additional materials on the bioassay platform to remove the excess microwave energy, which leads to an increase in the duration of microwave heating and in some cases evaporation of the small volume samples. In this regard, one can alleviate these issues using focused microwaves.

Focusing of microwaves to a specific region of interest, especially for small volume samples, can be accomplished by the use of metal-based mini-antennas with dimensions smaller than the wavelength of incident electromagnetic energy [8]. The mini-antennas focus the incident electric field to sharp edges of the mini-antennas, where up to a ~40,000-fold enhancement of the electric field is predicted [8]. Subsequently, the temperature of any solvent placed near the edges of the mini-antennas can be increased in a controlled manner. It was shown that one can extract biological materials from Anthrax spores by breaking down the walls of the spores by focused microwaves using aluminum mini-antennas fashioned into a "bow-tie" structure [9]. However, these mini-antennas were never employed in bioassays.

In the last decade, split ring resonator (SRR) structures have received a great amount of interest and were widely studied for the construction of metamaterials due to their unique interactions with electromagnetic energy [10]. SRR structures consists of concentric rings of a nonmagnetic metal (such as copper) separated by a gap (split). SRR structures are resonant around the magnetic plasma frequency [11–13] and magnetic field induces rotating currents in the rings. As a result, the rings produce their own flux, which enhances or dampens the incident field depending on the SRRs resonance properties [10]. SRR structures also exhibit an electric resonance by the dipole-like charge distribution along the incident electric field, which can be characterized by a band gap in the transmission spectrum of SRR. It is important to note that SRR structures that can focus enhanced electric field to a desired location can be designed using numerical simulations. There are commercially available software to carryout numerical

simulations to study the properties of transmission spectra [14–16], effective parameters [17–19], and the magnetic resonances of SRRs [11,20]. Several analytical models are reported for a better understanding of SRRs' resonance behavior [21–24]. The studies on SRRs and metamaterials are mainly performed in the gigahertz (GHz) frequency regime, but recently magnetic resonances of SRRs at terahertz (THz) frequencies have been obtained both experimentally and theoretically [25,26].

In this report, we report the results of a new bioassay technique that significantly improves the total assay time and the lower detection limit of colorimetric ELISA. The new bioassay technique is based on 1) the focusing of microwaves by SRR structures to a small volume micro-cuvette for uniform heating, 2) the creation of a thermal gradient between the assay medium and the silver nanoparticles for rapid completion of the bioassay steps. The SRR structures are made of copper thin films and have a single micro-cuvette (10 µl volume) in the split of the ring. Silver nanoparticles were covalently attached to the walls and the bottom of the micro-cuvette via amine groups of poly-L-lysine. The proof-of-principle of the new technique was demonstrated for a model protein, biotinylated-BSA. The identical ELISA was also carried out on commercially available HTS wells using room temperature incubation instead of microwave heating. While ELISA on HTS wells using room temperature took 70 min to complete, the identical ELISA was completed in < 2 min using new the technique, eliminating the need for longer incubation times. In addition, the lower detection limit of the colorimetric ELISA was improved ~100-fold by using SRR structures in combination with microwave heating and silver nanoparticles.

2 Materials and methods

2.1 Materials

Silver nitrate (>%99), D-glucose, ammonium hydroxide, sodium hydroxide, poly-L-lysine, biotinamidocaproyl-labeled bovine serum albumin (biotinylated-BSA), BSA, horse radish peroxidase (HRP)-labeled avidin, o-Phenylenediamine, hydrogen peroxide (%30), sulfuric acid, glass microscope slides and 96-well high throughput screening (HTS) plates with high protein binding capacity were purchased from Sigma-Aldrich Chemical Co. (Milwaukee, WI).

2.2 Methods-Construction and characterization of split-ring resonator (SRR) structures

The SRR structures are patterned on FR4 substrates ($2{\times}2$ cm^2) with a 30 µm thick copper layer. FR4 (National Electrical Manufacturers Association designation for circuit boards) is made from woven fiberglass with epoxy resin binder. The geometrical parameters of the SRR are $d = 3$ mm, $t = 0.9$ mm and $w = 9.4$ mm as shown in Figure 1A. The circuit board has a thickness 2.4 mm and dielectric constant of $\varepsilon = 3.85$. A single micro-cuvette with 10 µl volume capacity is drilled in the split of the SRR. Figure 1B shows the real-color photograph of a typical SRR structure.

Numerical simulations of the transmission spectrum of SRR structures were carried out to validate the use of SRR structures at 2.45 GHz. Simulations are carried out using a commercially available fullware solver, CST Microwave Studio® (Computer Simulation Technology AG), which employs finite integration method [13]. In the simulation setup, the structure is subjected to an incident plane wave. Open boundary conditions are employed along the propagation direction (the incident field propagates along the x-direction, with E and H along the y- and z-direction, respectively). The transmission amplitudes are obtained by using the fields at a distant point from the structures.

Transmission spectrum of the constructed SRR structures was also experimentally measured according to the previously published procedure [27]. In this regard, first, the transmission

spectrum in free space (i.e. without the SRR) was measured using monopole antennas and a HP-8510 C network analyzer. This spectrum was used to calibrate the network analyzer. The transmission spectrum of the SRR structures was measured by maintaining the distance between the transmitter and receiver monopole antennas. The length of the monopole antennas are λ/2, arranged to work at the frequency range covering the ω_m of the SRR structures.

2.3 Deposition of Silver Island Films (SIFs) inside the micro-cuvette of SRR structures

The micro-cuvettes were incubated with hydrogen peroxide for 5 min to oxidize the surface. Then, the surfaces were functionalized with amine groups by incubating a 10 µl aqueous solution of poly-lysine (5 % w/v) inside the micro-cuvettes for 2 hours. Unbound material was washed with deionized water. SIFs were deposited inside the micro-cuvette (bottom and the walls) using a modified version of the Tollen's reaction scheme. In this regard, first a solution of silver nitrate (0.5 g in 60 ml of deionized water) was placed in a clean 100-ml glass beaker. While stirring at the quickest speed, 200 L of freshly prepared 5 % (w/v) sodium hydroxide solution is added, which results in the formation of dark brown precipitates of silver particles. The precipitates were re-dissolved by ammonium hydroxide (2 ml). The resultant clear solution is cooled down to 5 °C by placing the beaker in an ice bath. After 2 min, a fresh solution of D-glucose (0.72 g in 15 ml of water) is added. Subsequently, a 10 µl portion of this mixture was transferred to the micro-cuvettes and the temperature of the mixture is then warmed to 40 °C by placing the SRR structures into pre-warmed laboratory oven (ThermoFisher, Model 280A). As the color of the mixture turns from yellow to green to green-brown (in 20 min), the mixture is removed from the micro-cuvettes. Subsequently, SIFs-deposited SRR structures were rinsed with deionized water several times and kept in air-tight dry containers until further use.

2.4 Construction of colorimetric ELISA on SRR structures and HTS plates with and without silver nanoparticles at room temperature and using microwave heating

In order to compare the efficiency (in terms of assay time and sensitivity) of SRR structures with the commercially available HTS plates, identical ELISA test for a model protein (b-BSA) was carried out on both the SRR structures using microwaves and on HTS plates at room temperature. In this regard, four different ELISA was constructed on SRR structures and HTS wells: 1) with SIFs and with microwave heating, 2) without SIFs and with microwave heating, 3) with SIFs and without microwave heating, 4) without SIFs and without microwave heating. Silver nanoparticles were deposited onto HTS wells using the previously published procedure [28].

Figure 2 shows the schematic depiction of the ELISA test used for b-BSA. In the first step, a solution of b-BSA with a range of bulk concentrations (1 µM to 1 pM) was incubated on SRR structures (10 µl) and HTS plates (100 µl) using low power microwave heating (Emerson Model no: MW8784SB, power input 1050W at 2.45 GHz, duty cycle = 3) for 10 seconds or at room temperature for 20 min, respectively. Unbound material was removed by rinsing with deionized water several times. The surfaces were then treated with 5 % (w/v) BSA to reduce the non-specific binding of avidin. In the next step, a 1 mg/ml solution of HRP-labeled avidin was incubated on SRR structures (10 seconds, microwave heating, duty cycle: 3) and HTS plates (20 min, room temperature). After washing off the unbound material by rinsing the surface with deionized water several times, a mixture of OPD and hydrogen peroxide was incubated on SRR structures (10 seconds, microwave heating, duty cycle: 3) and HTS plates (10 min, room temperature). The enzymatic reaction was stopped by the addition of 0.1 M sulfuric acid at the end of the indicated reaction times. Due to the intense color of the mixture on SRR structures and to measure the absorbance spectrum, this mixture was diluted and transferred to the HTS plates. The dilution of the mixture was done to ensure that the absorbance reading of all samples was less than 1. All experiments were repeated at least three times.

Scanning Electron Microscope (SEM) images of the micro-cuvettes of the SRR structures were obtained at the Core Imaging Facility of the University of Maryland Dental School.

3. Results and discussions

In order to employ SRR structures in biosensing applications using microwave heating, these structures have to be designed to function at the desired microwave frequency. Since most biosensing applications are based on water and water can be efficiently heated at 2.45 GHz using a conventional microwave oven, a SRR structure was designed that functions at 2.45 GHz. In this regard, first the SRR structures were characterized based on their transmission properties. It is well known that SRR structures have a strong response to electromagnetic (EM) wave due to magnetic resonance, which can be observed as a "dip" in the transmission spectrum of the SRR structure [29,30]. This can be attributed to the resonant nature of the SRR structures. Figure 3A shows the simulated and the experimental transmission spectrum for the SRR structures. Numerical simulations predict a dip in the transmission spectrum at 2.45 GHz, which is also experimentally observed, proving that the designed SRR structures function at 2.45 GHz. In addition, numerical calculations predict that the exposure of the SRR structures to an external magnetic field induces solenoidal current along the split ring (Figure 3B). That is, the SRR structure can be considered as a resonant magnetic dipole. The associated magnetic-field pattern from the SRR was previously shown to be dipolar [19].

In addition, the SRR structures are predicted to concentrate the incident electric field within the split in the ring. Figure 4 shows the simulated electric-field (total field) distribution along X–Y (Figure 4A) and Z-planes (Figure 4B) of the SRR structures. Figure 4A shows that electric fields are focused around the tips of the split in the ring, which was also shown for other metal-based mini-antennas [9]. This prediction can be explained in terms of short-circuiting the propagation of the incident electric field across the metal surface, such that charge builds up in the split of the ring, effectively localizing the microwaves to the micro-cuvette. In addition, the enhancement of incident electric field along the ring is also predicted, which is due to the excess charge buildup in the ring. One can manipulate the charge buildup by varying the magnitude and duration of the incident field. It is important to note that the micro-cuvette has a depth of 1mm, and the enhanced incident electric field on the X–Y plane crosses the top of micro-cuvette. That is, the incident electric field (in the X–Y plane) will be localized to the top of the micro-cuvette but not throughout the micro-cuvette. Subsequently, water placed in the micro-cuvette will not be effectively heated by the localized electric fields in the X–Y plane. Since the bioassays will be carried out only in the micro-cuvette, which has a volume of 10 µl, the electric field enhancement in the Z-plane is more relevant to the rapid heating of the solution placed in the micro-cuvette. As shown in Figure 4B, the electric field enhancement in the Z-plane is predicted to occur uniformly throughout the micro-cuvette extending into the entire micro-cuvette. Subsequently, the rapid and uniform heating of the solution placed in the micro-cuvette can be realized.

It is important to further comment on the nature of the micro-cuvette. The SRR structures were designed for bioassays that are required to process small volume samples. In this regard, two parameters were considered during the design of the SRR structures: 1) a micro-cuvette with a small-volume capacity that will reduce the assay time to a few seconds while yielding measurable absorption signal after the completion of the bioassays and 2) no loss of samples will occur due to low power microwave heating. It is also important to note that the walls and the bottom of the micro-cuvettes are modified with silver nanoparticles to create a thermal gradient between the solution and the surface of the silver nanoparticles where the bioassays are constructed. It was previously shown that the metal nanoparticles do not interact with the incident electric field due to their relatively small size (~80 nm) as compared to the wavelength of the microwaves (12.2 cm at 2.45 GHz) [5,31]. Subsequently, it is expected that the inclusion

of non-continuous silver nanoparticles inside the micro-cuvettes will not affect the electric field distribution, but play an important role in the creation of the thermal gradient.

It is also important to discuss the effect of the thermal gradient created between water and the silver nanoparticles on the overall efficiency of ELISA run on SRR structures. Figure 5 depicts the proposed mechanism for the increased rapidity and sensitivity of ELISA using low-power microwave heating and silver nanoparticles. In this regard, two distinct effects can be observed: Effect 1: upon exposure to microwave heating, a thermal gradient between water and silver nanoparticles is created due to the differences between their thermal conductivity (k) values. Since k values for water and FR4 substrate (and HTS wells) are similar, a thermal gradient is not expected to occur in the samples without silver nanoparticles. Thermal gradient between water and silver nanoparticles results in rapid mass transfer of b-BSA from the bulk to the surface of silver and subsequent rapid assembly of b-BSA on silver. Since b-BSA has NH_2-terminal groups and NH_2 groups have strong affinity towards silver surfaces the rapidly assembly process occurs preferentially on silver surface as previously shown [5]. Similarly, in the second step of ELISA, the rapid assembly of HRP-labeled on b-BSA modified surfaces occurs as a result of the thermal gradient and strong binding interactions between avidin and biotin groups. It was also previously shown that the non-specific interactions of avidin with the planar surfaces can be reduced when microwave heating is employed [5]. It is important to note that one BSA contains ~9 covalently-linked biotin molecules (from Sigma-Aldrich Corp.) and one BSA binds one avidin due to similar sizes of these proteins [32]. Subsequently, it is correct to assume that the extent of biotin molecules on BSA does not affect the extent of biorecognition events between avidin and b-BSA and the subsequent absorbance readout.

In Effect 2, microwave heating of assay components results in acceleration of the enzymatic conversion of o-Phenylenediamine (OPD) to a colored product in ~5 seconds. The identical enzymatic reaction takes a minimum of ~5–10 min to complete at room temperature. The observed increase in speed of enzymatic reaction using microwave heating is thought to be due to the availability of additional energy (microwave) for the conversion of OPD to the product. It was previously shown that microwave heating increases the rate of enzymatic reactions [33–35]. It was also shown that when exposed to microwaves the conversion of the non-luminescent organic substrates to luminescent products by HRP can be significantly increased [8,36]. In this regard, the use of low power microwaves increases the sensitivity of ELISA, where larger absorbance (or chemiluminescence) signals are obtained using microwave heating for the enzymatic conversion of the organic substrates, as compared to room temperature incubation.

Figure 6-Insets show the real-color photographs and SEM images of the SRR structures with and without silver nanoparticles present in the micro-cuvettes. SRR structures with mechanically drilled micro-cuvettes before the deposition of silver nanoparticles have the same color of the FR4 substrate, which is composed of fiber glass and epoxy resin. After the deposition of silver nanoparticles, the color of the surface of micro-cuvette was changed to the color of silver nanoparticles (green-brown). The color of silver nanoparticles deposited onto surfaces depends on the loading and the size of the nanoparticles themselves. According to our procedure silver nanoparticles are allowed to grow for 20 min at 40 °C, which resulted in higher loading density of silver nanoparticles as compared to a typical SIFs surface used for other applications [5]. SEM images of the SRR structures reveal the heterogeneous nature of the micro-cuvette of the SRR structures with smooth ridges and valleys (Figure 6A). After the deposition of SIFs, the smooth surfaces of the micro-cuvette are covered with individual and small aggregates of silver nanoparticles (Figure 6B). A high-magnification SEM image of the micro-cuvette reveals that size of the silver nanoparticles is ~150 nm. As expected, the size of the SIFs in this study is larger than those used in other applications due to the longer incubation times (20 min vs 2 min) [5].

The criteria for the extent of loading of silver nanoparticles in the present study are: 1) retaining the split in the ring (so that the circuit of the ring is not completed and 2) providing the largest amount of surface area (of silver nanoparticles) for the construction of the bioassays. In this regard, SIFs have to be deposited inside the micro-cuvette of the SRR structures in a noncontinuous fashion. It should be noted that one can only control the extent of loading (i.e. inter-island spacing) of the SIFs by changing the incubation time of reduced silver nitrate solution due to the nature of Tollen's reaction scheme. Alternatively, spherical silver nanoparticles (prepared separately) can be deposited inside the micro-cuvette of the SRR structures by simple incubation. The disadvantages of the latter method are: longer incubation times and multiple incubations are required to obtain the desired loading of silver nanoparticles. Moreover, the deposition of thin metal films (continuous surface) inside the micro-cuvette would complete the circuit and the SRR structures would be unusable for biosensing applications. It is important to note that ELISA based on absorbance-readout is investigated in the present study. Subsequently, the effect of silver nanoparticles on the absorbance is not sought as one would do in metal-enhanced fluorescence based biosensing scheme [5].

A series of experiments were carried out to investigate the effect of using SRR structures, microwaves and silver nanoparticles on ELISA tests. Commercially available 96-well HTS plates (referred to as HTS wells) were employed to directly compare the efficiency of new SRR structures in terms of total assay time and sensitivity with the "gold standard" for ELISA tests, which are HTS wells. In this regard, ELISA tests using SRR structures and HTS wells were carried out in four different categories: SRR structures and HTS wells 1) with SIFs and with microwave heating, 2) without SIFs and with microwave heating, 3) with SIFs and without microwave heating, 4) without SIFs and without microwave heating.

Figure 7 shows the results of these experiments and control experiments, where the normalized absorbance at 450 nm for OPD (to the largest value observed: 10^{-6} M for ELISA denoted as "MW, SRR with SIFs, 2 min") was plotted against concentration of b-BSA in solution. In control experiments, where b-BSA is omitted from the surface, the background signal (horizontal lines) is measured to determine the lower detection limit for ELISA using both the SRR structures and HTS wells. Figure 7A shows the direct comparison of the results of ELISA for b-BSA run using "gold standard" HTS wells with and without silver nanoparticles, using low-power microwave heating and at room temperature. In ELISA carried out on HTS wells with SIFs at room temperature, which took 70 min to complete, the detectable concentration range for b-BSA was ~1 nM – 0.1 µM. A similar detectable concentration range for b-BSA is observed when SIFs were omitted from the HTS wells, which implies that the use of SIFs alone in ELISA run at room temperature have no or little effect on the sensitivity of ELISA. It was previously shown that the incorporation of microwave heating into fluorescence-based bioassays run on HTS wells with SIFs, results in significant reduction in assay time [28]. In this regard, the identical ELISA on HTS wells with SIFs was repeated using microwave heating instead of room temperature incubation steps. The total assay time was reduced to 2 min using microwave heating and the assay sensitivity was similar to ELISA run at room temperature (Figure 7A-"MW, HTS with SIFs, 2 min"). That is, one can employ microwave heating and silver nanoparticles in absorbance-based ELISA to complete the assay in a fraction of the time for conventional ELISA using the same HTS wells with the addition of silver deposition step. The deposition of silver nanoparticles onto HTS wells was shown to be highly reproducible [28]. On the other hand, the incorporation of microwave heating to conventional ELISA without silver nanoparticles results in poor sensitivity (Figure 7A- "MW, HTS without SIFs, 2 min"). These observations provide direct evidence that the incorporation of microwave heating into incubation steps results in rapid assembly of proteins (Effect 1 in Figure 5).

Figure 7B shows the direct comparison of the results of ELISA for b-BSA run using the new SRR structures with and without silver nanoparticles, using low-power microwave heating and

at room temperature. Using SRR structures with low-power microwaves heating and with silver nanoparticles (Figure 7B-"MW, SRR with SIFs, 2 min"), the identical ELISA run at room temperature was completed in 2 min and the lower detection limit for b-BSA is improved by 100-fold (0.01 nM). That is, the lower detection limit for the absorbance-based ELISA is now approaching the sensitivity of ELISA based on chemiluminescence detection scheme, which is a significant improvement of the current absorbance-based bioassays. Subsequently, the effect of concomitant use of microwave heating and silver nanoparticles in ELISA run SRR structures was also investigated. First, silver nanoparticles were omitted from the SRR structures and the identical ELISA was completed using microwave heating (Figure 7B-"MW, SRR without SIFs, 2 min"). A significant decrease in absorbance values for the concentration range for b-BSA was observed, which was similar to those observed for HTS wells (Figure 7A-"MW, HTS without SIFs, 2 min"). These observations can be attributed to the absence of the thermal gradient on SRR structures and HTS wells without silver nanoparticles (thermal conductivity of water and the SRR structures and HTS wells are similar), where a high thermal conductivity material is required for the creation of the thermal gradient. While only silver nanoparticles are employed in this study, it is important to note that other metal nanoparticles with high thermal conductivity can also be employed. In this regard, one has to ensure the reproducible deposition of the metal nanoparticles onto the SRR structures. Next, ELISA was run on SRR with and without silver nanoparticles (Figure 7B-"RT, SRR with/without SIFs, 70 min"), where the incubation steps were carried out at room temperature instead of microwave heating. A 40 % decrease in absorbance values for the concentration range for b-BSA as compared to ELISA run on SRR with microwave heating and silver nanoparticles was observed. These observations provide indirect evidence that microwave heating increases the efficiency of enzymatic reactions (Effect 2 in Figure 5).

Figure 8 shows the comparison of normalized absorbance measured from ELISA (10^{-6} M b-BSA) run on HTS wells and SRR structures with and without SIFs using microwave heating. One can infer the following from Figures 7 and 8:

1. Absorbance values for ELISA run on HTS wells with or without silver nanoparticles at room temperature are similar. That is, the incorporation of silver nanoparticles into absorbance-based ELISA run at room temperature has no or little effect on the sensitivity of ELISA (Figure 8A). This also implies that the addition of silver nanoparticles to the surfaces do not increase the loading of the proteins on the surfaces.

2. The incorporation of microwave heating steps into ELISA run on HTS wells with and without silver nanoparticles does not improve the sensitivity of ELISA. One can complete the absorbance-based ELISA on HTS wells in 2 min using silver nanoparticles and microwave heating, while slightly sacrificing assay sensitivity (Figure 8A).

    2.1) Faster assay time on HTS wells with silver nanoparticles is attributed to the rapid assembly of proteins by due to the thermal gradient created by the incorporation of microwave heating into incubation steps (Effect 1 in Figure 5).

    2.2) Although the absorbance values for microwave heating-based ELISA on HTS wells with and without silver nanoparticles are lower than ELISA run at room temperature, one cannot rule out the effect of microwave heating on the efficiency of enzymatic reactions in HTS wells. Due to the complexity of these experiments, the effect of microwave heating on the efficiency of enzymatic reactions in HTS wells was not inferred from the results. One major factor is the size and shape of the HTS wells: HTS wells are significantly large in size (comparable to the wavelength of microwave

energy at 2.45 GHz (12.2 cm) and have sharp edges, which can result in inefficient heating of samples.

3. ELISA run on SRR structures with silver nanoparticles and microwave heating yields larger absorbance values than those from HTS wells (Figure 8B). This is attributed to the focusing of microwave energy to a small volume micro-cuvette by SRR structures, which increases the efficiency of enzymatic reactions (Effect 2 in Figure 5). In addition, ELISA can be completed in 2 min due to the presence of thermal gradient resulting in the rapid assembly of proteins (Effect 1 in Figure 5).

4. ELISA run on SRR structures without silver nanoparticles and with microwave heating yields significantly lower absorbance values (Figure 8B), due to the absence of the thermal gradient as also observed with the HTS wells.

5. ELISA run on SRR structures with and without silver nanoparticles at room temperature yields lower absorbance values (Figure 8B), partially proving the point that microwave heating increases the efficiency of enzymatic reactions (Effect 2 in Figure 5).

It is also important to comment on the nature of the biotin-avidin interactions used in this study. Biotin-avidin interactions are one of the strongest biological interactions in nature [32], and are typically employed in proof-of-principle demonstration of new assay techniques [5,37, 38]. The biotin-avidin interactions typically reach >95% completion in 10–20 min for all concentrations [39] and subsequently we did not seek longer incubation times. The idea of using microwave heating with silver nanoparticles for lower-affinity biological interactions such as antigen-antibody [40] and DNA hybridization assays [41,42] were demonstrated previously. In this regard, the authors believe that the use of SRR structures with silver nanoparticles and microwave heating for immunoassays that employs low-affinity biological interactions are also expected to work as efficiently as the bioassay tested in the present study. Indeed, we are currently working on increasing the number of samples that can be tested at once by designing new SRR-structures containing multiple micro-cuvettes for immunoassays. These results will be reported in due course.

4. Conclusions

In this paper, we have reported a new approach to commercially available colorimetric ELISA demonstrating that the total assay time and lower detection limit of ELISA can be significantly improved. The new approach included the design and use of electrically small SRR structures to focus low-power microwaves to a small volume micro-cuvette containing silver nanoparticles, where the bioassay was constructed. The design of the SRR structures was carried out by numerical simulations to show these structures can function at the frequency of a common microwave oven (2.45 GHz), which were also confirmed by experimental transmission studies. Silver nanoparticles were covalently attached to the bottom and the walls of the micro- cuvette in a way that the presence of silver nanoparticles did not result in completion of the circuit in the SRR structures. Silver nanoparticles were used to create a thermal gradient between the water and their surfaces, effectively driving the HRP-labeled avidin in the relatively warmer water to the surface of silver nanoparticles containing b-BSA. While the bioassay for the detection of b-BSA took 70 min to complete on HTS wells at room temperature, the identical bioassay was completed within 2 min using low-power microwave heating and the silver nanoparticle-modified SRR structures. The importance of shorter assay times lies in the fact that researchers can now run ELISA "on-demand" without having to wait for the completion of incubation steps. The detectable concentration range for b-BSA was ~1 nM – 0.1 µM and ~0.01 nM – 0.1 µM for ELISA run at room temperature (HTS plates) and with microwave heating (SRR structures), respectively. A 100-fold improvement of the lower detection limit for b-BSA using SRR structures over HTS plates is observed.
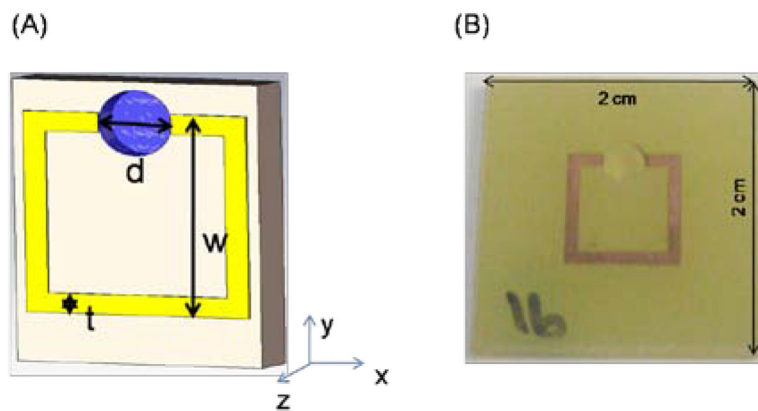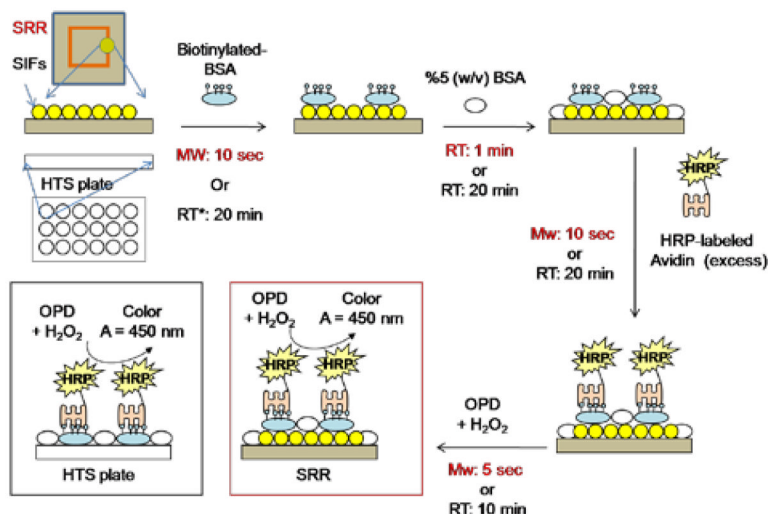
Acknowledgments

References

1. Chuang KH, Tzou SC, Cheng TC, Kao CH, Tseng WL, Shiea J, Liao KW, Wang YM, Chang YC, Huang BJ, Wu CJ, Chu PY, Roffler SR, Cheng TL. Measurement of Poly(ethylene glycol) by Cell-Based Anti-poly(ethylene glycol) ELISA. Analytical Chemistry 2010;82:2355–2362. doi:10.1021/ac902548m. [PubMed: 20178318]

2. Samineni S, Parvataneni S, Kelly C, Gangur V, Karmaus W, Brooks K. Optimization, comparison, and application of colorimetric vs. chemiluminescence based indirect sandwich ELISA for measurement of human IL-23. Journal of Immunoassay & Immunochemistry 2006;27:183–193. doi: 10.10 80/15321810600573051. [PubMed: 16711255]

3. Jablonski JE, Fu TJ, Jackson LS, Gendel SM. Determination of Protein Levels in Soy and Peanut Oils by Colorimetric Assay and ELISA. Journal of Aoac International 2010;93:213–220. [PubMed: 20334183]

4. Sapsford KE, Francis J, Sun S, Kostov Y, Rasooly A. Miniaturized 96-well ELISA chips for staphylococcal enterotoxin B detection using portable colorimetric detector. Analytical and Bioanalytical Chemistry 2009;394:499–505. doi:10.1007/s00216-009-2730-z. [PubMed: 19290511]

5. Aslan K, Geddes CD. Microwave-accelerated metal-enhanced fluorescence: Platform technology for ultrafast and ultrabright assays. Analytical Chemistry 2005;77:8057–8067. doi:10.1021/ac0516077. [PubMed: 16351156]

6. Aslan K, Geddes CD. New tools for rapid clinical and bio-agent diagnostics: microwaves and plasmonic nanostructures. Analyst 2008;133:1469–1480. doi:10.1039/b808292h. [PubMed: 18936822]

7. Aslan K, Gryczynski I, Malicka J, Matveeva E, Lakowicz JR, Geddes CD. Metal-enhanced fluorescence: an emerging tool in biotechnology. Current Opinion in Biotechnology 2005;16:55–62. doi:10.1016/j.copbio.2005.01. 001. [PubMed: 15722016]

8. Previte MJR, Aslan K, Geddes CD. Spatial and temporal control of microwave triggered chemiluminescence: A protein detection platform. Analytical Chemistry 2007;79:7042–7052. doi: 10.1021/ac071042+ [PubMed: 17696497]

9. Aslan K, Previte MJ, Zhang Y, Gallagher T, Baillie L, Geddes CD. Extraction and detection of DNA from Bacillus anthracis spores and the vegetative cells within 1 min. Analytical Chemistry 2008;80:4125–4132. doi:10.1021/ac800519r. [PubMed: 18459738]

10. Pendry JB, Holden AJ, Robbins DJ, Stewart WJ. Low frequency plasmons in thin-wire structures. Journal of Physics-Condensed Matter 1998;10:4785–4809. doi:10.1088/0953-8984/10/22/007.

11. Gay-Balmaz P, Martin OJF. Electromagnetic resonances in individual and coupled split-ring resonators. Journal of Applied Physics 2002;92:2929–2936. doi:10.106 3/1.1497452.

12. Pendry JB, Holden AJ, Robbins DJ, Stewart WJ. Magnetism from conductors and enhanced nonlinear phenomena. Ieee Transactions on Microwave Theory and Techniques 1999;47:2075–2084. doi: 10.1109/22.798002.

13. Smith DR, Padilla WJ, Vier DC, Nemat-Nasser SC, Schultz S. Composite medium with simultaneously negative permeability and permittivity. Physical Review Letters 2000;84:4184–4187. doi:10.1103/PhysRevLett.8 4.4184. [PubMed: 10990641]

14. Markos P, Soukoulis CM. Numerical studies of left-handed materials and arrays of split ring resonators. Physical Review E 2002;65:-.

15. Markos P, Soukoulis CM. Transmission properties and effective electromagnetic parameters of double negative metamaterials. Optics Express 2003;11:649–661. doi:10.1364/OE.11.000649. [PubMed: 19461777]

16. Ziolkowski RW. Design, fabrication, and testing of double negative metamaterials. Ieee Transactions on Antennas and Propagation 2003;51:1516–1529. doi:10.1109/TAP.2003.813622.

17. Katsarakis N, Koschny T, Kafesaki M, Economou EN, Soukoulis CM. Electric coupling to the magnetic resonance of split ring resonators. Applied Physics Letters 2004;84:2943–2945. doi: 10.1063/1.1695439.

18. Koschny T, Kafesaki M, Economou EN, Soukoulis CM. Effective medium theory of left-handed materials. Physical Review Letters 2004;93:-.

19. Koschny T, Markos P, Smith DR, Soukoulis CM. Resonant and antiresonant frequency dependence of the effective parameters of metamaterials. Physical Review E 2003;68:-.

20. Hsu YJ, Huang YC, Lih JS, Chern JL. Electromagnetic resonance in deformed split ring resonators of left-handed meta-materials. Journal of Applied Physics 2004;96:1979–1982. doi: 10.1063/1.1767290.

21. Baena JD, Marques R, Medina F, Martel J. Artificial magnetic metamaterial design by using spiral resonators. Physical Review B 2004;69:-.

22. Marques R, Mesa F, Martel J, Medina F. Comparative analysis of edge- and broadside-coupled split ring resonators for metamaterial design - Theory and experiments. Ieee Transactions on Antennas and Propagation 2003;51:2572–2581. doi:10.1109/TAP.2003.817562.

23. Sauviac B, Simovski CR, Tretyakov SA. Double split-ring resonators: Analytical modeling and numerical simulations. Electromagnetics 2004;24:317–338. doi:10.1080/02726340490457890.

24. Shamonin M, Shamonina E, Kalinin V, Solymar L. Properties of a metamaterial element: Analytical solutions and numerical simulations for a singly split double ring. Journal of Applied Physics 2004;95:3778–3784. doi:10.1063/1.1652251.

25. Linden S, Enkrich C, Wegener M, Zhou JF, Koschny T, Soukoulis CM. Magnetic response of metamaterials at 100 terahertz. Science 2004;306:1351–1353. doi:10.1126/science.1105371. [PubMed: 15550664]

26. Yen TJ, Padilla WJ, Fang N, Vier DC, Smith DR, Pendry JB, Basov DN, Zhang X. Terahertz magnetic response from artificial materials. Science 2004;303:1494–1496. doi:10.1126/science.1094025. [PubMed: 15001772]

27. Caglayan H, Ozbay E. Surface wave splitter based on metallic gratings with sub-wavelength aperture. Optics Express 2008;16:19091–19096q. doi:10.1364/OE.16.019091. [PubMed: 19582001]

28. Aslan K, Holley P, Geddes CD. Microwave-Accelerated Metal-Enhanced Fluorescence (MAMEF) with silver colloids in 96-well plates: Application to ultra fast and sensitive immunoassays, High Throughput Screening and drug discovery. Journal of Immunological Methods 2006;312:137–147. doi:10.1016/j.jim.2006.03.009. [PubMed: 16678196]

29. Aydin K, Guven K, Katsarakis N, Soukoulis CM, Ozbay E. Effect of disorder on magnetic resonance band gap of split-ring resonator structures. Optics Express 2004;12:5896–5901. doi:10.1364/OPEX. 12.005896. [PubMed: 19488229]

30. Movchan AB, Guenneau S. Split-ring resonators and localized modes. Physical Review B 2004;70:-.

31. Aslan K, Geddes CD. Microwave-accelerated ultrafast nanoparticle aggregation assays using gold colloids. Analytical Chemistry 2007;79:2131–2136. doi:10.1021/ac0620967. [PubMed: 17256878]

32. Green NM. Advanced Protein Chemistry 1975;29:85–133. doi:10.1016/S0065-3233(08)60411-8.

33. Leadbeater NE, Stencel LM, Wood EC. Probing the effects of microwave irradiation on enzyme-catalysed organic transformations: the case of lipase-catalysed transesterification reactions. Org Biomol Chem 2007;5:1052–1055. doi:10.1039/b617544a. [PubMed: 17377658]

34. Lin SS, Wu CH, Sun MC, Sun CM, Ho YP. Microwave-assisted enzyme-catalyzed reactions in various solvent systems. J Am Soc Mass Spectrom 2005;16:581–588. doi:10.1016/j.jasms. 2005.01.012. [PubMed: 15792728]

35. Mazumder S, Laskar DD, Prajapati D, Roy MK. Microwave-induced enzyme-catalyzed chemoselective reduction of organic azides. Chem Biodivers 2004;1:925–929. doi:10.1002/cbdv. 200490074. [PubMed: 17191892]

36. Previte MJ, Aslan K, Malyn SN, Geddes CD. Microwave triggered metal enhanced chemiluminescence: quantitative protein determination. Anal Chem 2006;78:8020–8027. doi: 10.1021/ac061161+ [PubMed: 17134135]

37. Aslan K. Rapid Whole Blood Bioassays using Microwave-Accelerated Metal-Enhanced Fluorescence. Nano Biomedicine and Engineering 2010;2:1–9. doi:10.5101/nbe.v2i1.p1-7. [PubMed: 20622988]
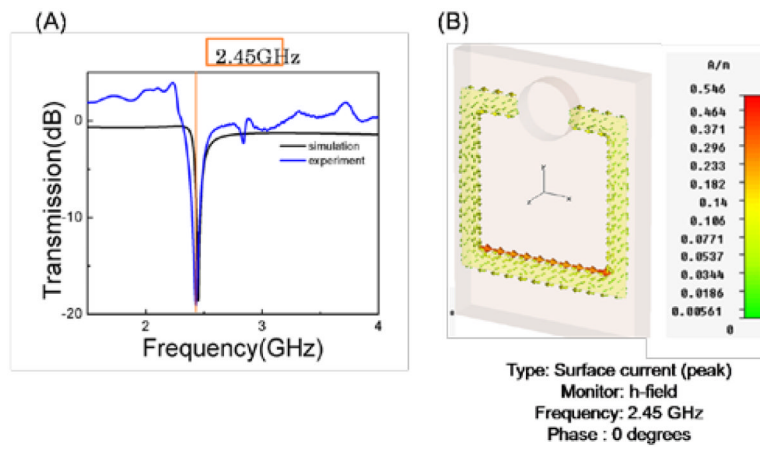
38. Aslan, K.; Gryczynski, I.; Malicka, J.; Lakowicz, JR.; Geddes, CD. Metal-Enhanced Fluorescence: Application to High-Throughput Screening and Drug Discovery. In: Gad, S., editor. Drug Discovery Handbook. New Jersey: Wiley & Sons; 2005. doi:10.1002/0471728780.ch14

39. Aslan K, Luhrs CC, Perez-Luna VH. Controlled and reversible aggregation of biotinylated gold nanoparticles with streptavidin. Journal of Physical Chemistry B 2004;108:15631–15639. doi: 10.1021/jp036089n.

40. Aslan K, Geddes CD. Microwave Accelerated and Metal Enhanced Fluorescence Myoglobin Detection on Silvered Surfaces: Potential Application to Myocardial Infarction Diagnosis. Plasmonics 2006;1:53–59. doi:10.1007/s11468-006-9006-7. [PubMed: 19444320]

41. Aslan K, Malyn SN, Bector G, Geddes CD. Microwave-accelerated metal-enhanced fluorescence: an ultra-fast and sensitive DNA sensing platform. Analyst 2007;132:1122–1129. doi:10.1039/b708069g. [PubMed: 17755146]

42. Aslan K, Zhang YX, Hibbs S, Baillie L, Previte MJR, Geddes CD. Microwave-accelerated metal-enhanced fluorescence: application to detection of genomic and exosporium anthrax DNA in < 30 seconds. Analyst 2007;132:1130–1138. doi:10.1039/b707876e. [PubMed: 17955147]
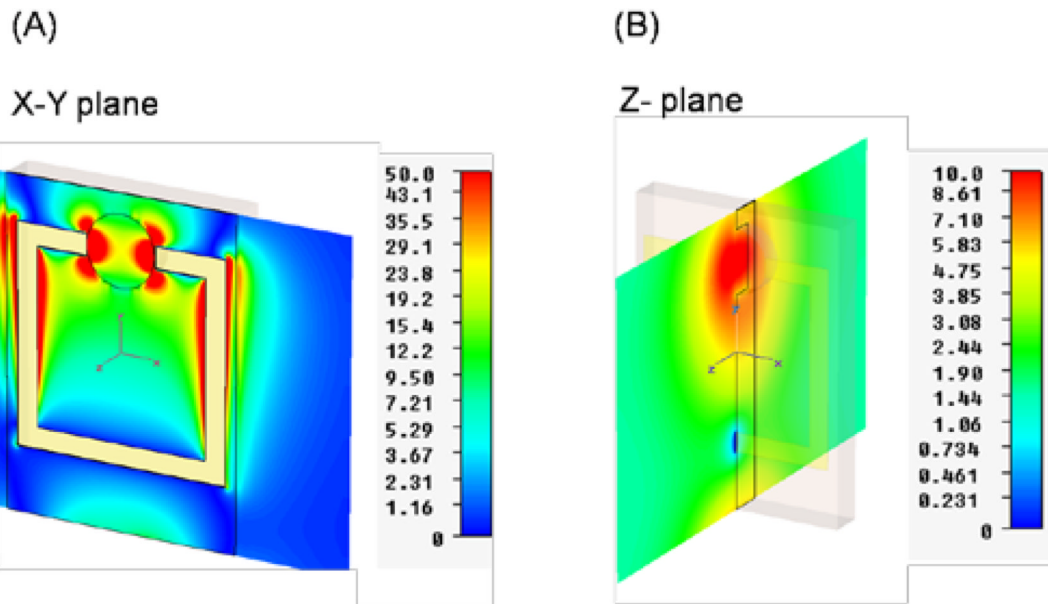
Figure 1.
(A) Schematic depiction of copper split ring resonator (SRR) structures printed on a circuit board. The dimensions of the SRR structures are d = 3 mm, t = 0.9 mm and w = 9.4 mm. A single micro-cuvette (depth = 1 mm) is drilled in the split of the SRR and has a 10 µl volume capacity. (B) Real-color photographs of SRR structures.

Figure 2.
Schematic depiction of the Enzyme-Linked Immunosorbent Assay (ELISA) for the detection of the model protein (biotinylated-BSA) used in this study.

*Control experiments were carried out in a commercially available 96-well high throughput screening (HTS) plates without SIFs. SRR: Split ring resonator structures; SIFs: Silver island films; BSA: Bovine serum albumin; HRP: horse radish peroxidase; OPD: o-Phenylenediamine; RT: Room temperature; MW: Low-power microwave heating; A: Absorbance.
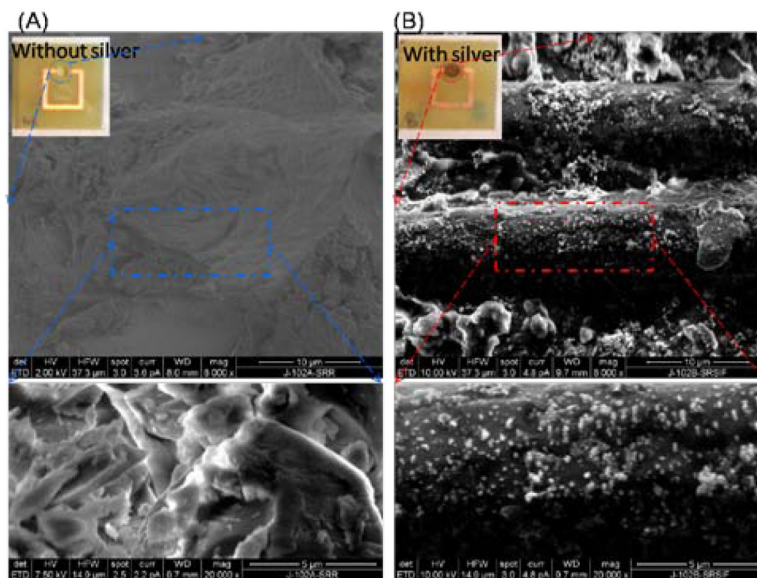
Figure 3.
(A) Simulated and experimental transmission spectrum for SRR structures. (B) Calculated charge distribution along the SRR structures.
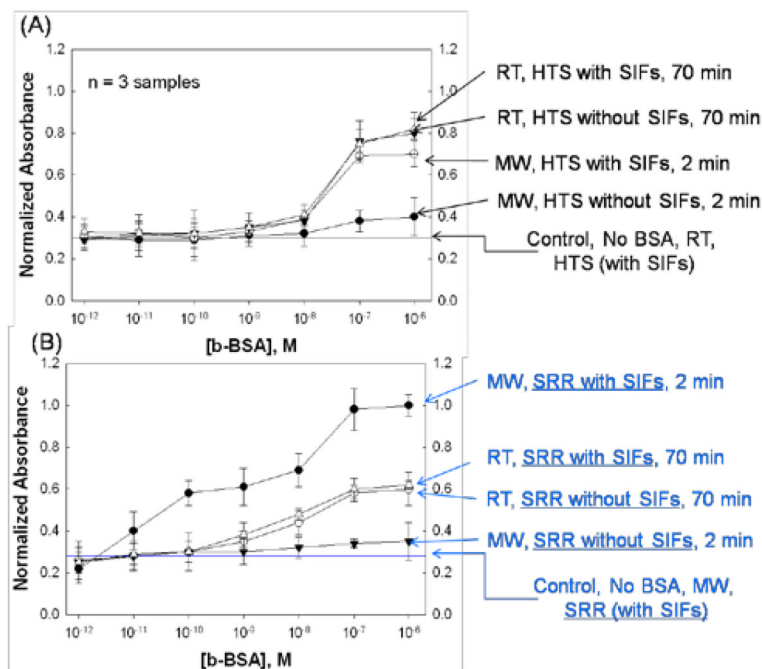
(A)

X-Y plane

(B)

Z- plane

Figure 4.
Simulated electric field enhancements for SRR structures (A) X–Y plane and (B) Z-plane. The scales displayed to the right of the figures represent the magnitude of the electric field intensity distribution in the respective dimensions.

Figure 5.
Schematic depiction of the proposed mechanism for the increased rapidity and sensitivity of ELISA using low-power microwave heating and silver nanoparticles. Effect1: Upon exposure to microwave heating, a thermal gradient between water and silver nanoparticles is created due to the differences between their thermal conductivity (k) values. Since k values for water and FR4 substrate are similar, a thermal gradient is not expected to occur in the samples without silver nanoparticles. Thermal gradient between water and silver nanoparticles results in rapid mass transfer of b-BSA from the bulk to the surface of silver and subsequent rapid assembly of b-BSA on silver. Effect 2: microwave heating accelerates the enzymatic conversion of o-Phenylenediamine (OPD) to a colored product.
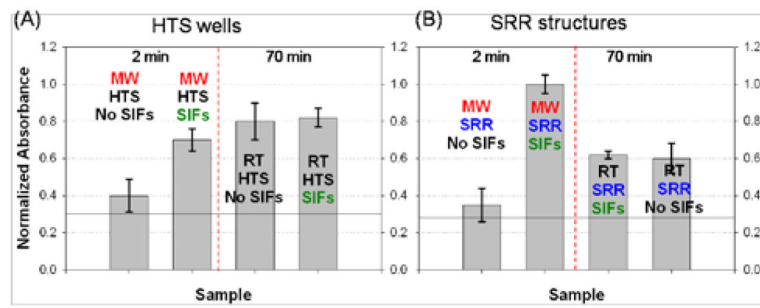
Figure 6.
Scanning Electron Microscope (SEM) images of the micro-cuvettes of the SRR structures (A) before and (B) after the deposition of SIFs. SIFs were deposited at the same time using Tollen's reaction scheme. SIFs were covalently linked to polylysine groups inside the micro-cuvettes and did not detach from the surface after the completion of the bioassays.

Figure 7.
Normalized absorbance at 450 nm for OPD after the completion of ELISA for the detection of b-BSA using (A) SRR structures (with SIFs) and microwaves and HTS wells (without SIFs) at room temperature and (B) control experiments. The absorbance values were normalized to the largest value observed: 10^{-6} M for ELISA denoted as "MW, SRR with SIFs, 2 min". The average absorbance values for 3 different runs are shown. In the control experiment, b-BSA was omitted from the surface to determine the detectable concentration range using both methods.

Figure 8.
The comparison of normalized absorbance measured from ELISA (10^{-6} M b-BSA) run on (A) HTS wells and (B) SRR structures with and without SIFs using microwave heating (MW).